Numerical Study on Characteristics of Ship Wave According to Shape of Waterway Section

Chun-Beom Hong*
Marine Research Institute, Samsung Heavy Industries Co., Daejeon 305-380, Korea
Sang-Min Lee
Research Institute of Maritime Industry, Korea Maritime University, Pusan 606-791, Korea

The ship wave phenomena in the restricted waterway were investigated by a numerical analysis. The Euler and continuity equations were employed for the present study. The boundary fitted and moving grid system was adopted to enhance the computational efficiency. The convective terms in the governing equations and the kinematic free surface boundary condition were solved by the Constrained Interpolated Profile (CIP) algorithm in order to solve accurately wave heights in far field as well as near field. The advantage of the CIP method was verified by the comparison of the computed results by the CIP and the Maker and Cell (MAC) method. The free surface flow simulation around Wigley hull was performed and compared with the experiment for the sake of the validation of the numerical method. The present numerical scheme was applied to the free surface simulation for various canal sections in order to understand the effect of the sectional shape of waterways on the ship waves. The wave heights on the side wall and the shape of the wave patterns with their characteristics of flow are discussed.

Key Words : Ship Wave, Shallow Water, Waterway, Constrained Interpolated Profile (CIP) Algorithm

1. Introduction

Increase of transportation using inland waterways inspires investigations of ship waves in restricted and shallow waterways. Especially environmental issues regarding the bank erosion caused by the passage of ships in a river reported by Fukuoka et al.(2000). The erosion of beach caused by divergent waves from the vessels is the recent topics. In the present time, wash, noise, and environmental pollution are considered as fundamental ship design criteria in the same way that ship speed, deadweight capacity, passenger accommodation, and maneuverability have been part of the ship design criteria. A ship cruising in a shallow waterway gives adverse effects on the coastal environment through the generation of significant wash. These effects include erosion or deformation of the beach and bank, damage to structures, people, and vessels around the beach. A wider viewpoint on the wash can be found from the UK Maritime and Coastguard Agency (2001) report, in which several recommendations were given focusing on the wash characteristics and the hull form to minimize the wave energy. Whittaker et al.(2001) and Doyle et al.(2001) mentioned that the decay ratio of wave height becomes smaller as the water becomes shallower. Doctors et al.(2001) studied the optimization of the hull parameter by taking into account of the wash effect. However, most of the researchers

* Corresponding Author,
E-mail : cb.hong@samsung.com
TEL : +82-42-865-4782; **FAX** : +82-42-865-4380
Marine Research Institute, Samsung Heavy Industries Co., Daejeon 305-380, Korea. (Manuscript **Received** March 15, 2005; **Revised** November 8, 2005)

have concerned only on the ship wave in shallow water with a constant water depth, not with arbitrary water depth. The present study focuses on the characteristics of the ship waves according to the shapes of the waterway section, which is significant factors to change the form of waves.

Numerical analysis, including the free surface motion, is crucial in order to understand the characteristics of ship waves near the shore. Being a solution of the initial and nonlinear boundary condition, the location of free surface is one of the most difficult solutions to obtain. The numerical method using the Maker and Cell (MAC) method developed by Welch et al.(1966) has been used for the simulation of the nonlinear wave phenomena. Kwag (2000) and Kong(2005) applied the MAC method to the analysis of ship wave but there was a requirement for expensive computational effort for high accurate solution in far field. In order to simulate the flow field precisely, Xiao et al.(1999) developed Constrained Interpolated Profile (CIP) method, which can resolve the behavior of solution inside grid cell. The numerical method was used for various engineering problem (Yabe et al., 1996 ; Watanabe et al., 1999) and showed good results in the propagated waves particularly. In this study, CIP method was applied to analyze the ship waves. The calculated waves by CIP method and MAC method were compared to discuss the computational resolution.

2. Governing Equations

Three-dimensional incompressible Euler and continuity equations are employed for the present numerical simulation of ship waves. The non-dimensional form of the governing equations is expressed as follows,

$$\frac{\partial u}{\partial \tau}+u\frac{\partial u}{\partial x}+v\frac{\partial u}{\partial y}+w\frac{\partial u}{\partial z}=-\frac{\partial p}{\partial x} \tag{1}$$

$$\frac{\partial v}{\partial \tau}+u\frac{\partial v}{\partial x}+v\frac{\partial v}{\partial y}+w\frac{\partial v}{\partial z}=-\frac{\partial p}{\partial y} \tag{2}$$

$$\frac{\partial w}{\partial \tau}+u\frac{\partial w}{\partial x}+v\frac{\partial w}{\partial y}+w\frac{\partial w}{\partial z}=-\frac{\partial p}{\partial z} \tag{3}$$

$$\nabla\cdot\vec{v}=0 \tag{4}$$

where $p=p^*+\frac{z}{Fn^2}$, $p^*=p^{**}-p_{air}$ and $F_n=\frac{U_0}{\sqrt{gL}}$. x, y and z are the Cartesian coordinates system fixed on the model ship. x and z are the longitudinal and vertical axes while y designates the lateral axis from the center plane of the ship model. The origin of axis is located at the intersection of the calm water plane and the midship of the model. τ is the non-dimensional time in fixed computational domain. u, v and w are the velocity component in x, y and z directions. $\vec{v}$ denotes velocity vector. p, p^{**}, p_{air}, U_0, g and L indicate the modified pressure, the pressure, the atmospheric pressure, the uniform flow velocity, the gravity acceleration, and the ship length, respectively. All variables in the governing equations are non-dimensionalized by the ship length and the uniform flow velocity.

3. Boundary Conditions

Neglecting the effects of surface tension and viscosity, the pressure acting on the free surface is set to be the atmospheric pressure as shown in equation (5). The velocity of fluid on the free surface must satisfy the kinematic boundary condition as shown in equation (6).

$$p^*=p_{air} \tag{5}$$

$$\frac{\partial \zeta}{\partial \tau}=w-u\frac{\partial \zeta}{\partial x}-v\frac{\partial \zeta}{\partial y} \tag{6}$$

where $\zeta(x, y, t)$ is the wave height.

Free slip boundary condition is used for the wall boundary proposed by Hung (1987). The velocity boundary condition on the wall is given as follows,

$$\vec{v}\cdot\vec{n}=0 \tag{7}$$

$$\frac{\partial V_t}{\partial_n}=0 \tag{8}$$

where, V_t is the tangential velocity component. The unit vector normal to the wall is denoted by $\vec{n}$. The pressure boundary condition on the body surface is derived to satisfy the momentum equation. On the upstream boundary of the computational domain, uniform flow condition is applied,

while zero gradient condition is given on the outer boundary. On the center plane, the symmetric boundary condition is applied.

4. Numerical Scheme

4.1 CIP method

In the present study, the CIP method is employed for three dimensional ship wave simulation in the curvilinear coordinate system. The discretized forms of the governing equations are split into two stages, non-advection and advection stage, assuming a small time increment.

In the non-advection stage, $\vec{v}^*$ and ζ^* are calculated by equations (9) and (10).

$$\frac{\vec{v}^*-\vec{v}^m}{\Delta t}=-\nabla p^m \tag{9}$$

$$\frac{\zeta^*-\zeta^m}{\Delta t}=w^m \tag{10}$$

where superscripts $*$ and m denote time step in non-advection stage and Δt means time increment. Taking the divergence of equation (9), Poisson equation for pressure can be derived.

$$\nabla^2 p^*=-\frac{D^m}{\Delta t} \tag{11}$$

where D represents the divergence of velocity vector. Equations (9), (10) and (11) are transformed into a body fitted coordinate system and discretized by finite difference method with the second order accuracy.

Once $\vec{v}^*$ and p^* are obtained in non-advection stage, the CIP method, which can express the behavior of the solution and its derivatives inside grid cell, is applied to the calculation of the flow advection.

The function (f), such as velocity component or wave elevation, and its derivatives $(\partial f/\partial \xi_i)$ are expressed by cubic polynomial in curvilinear coordinate system as shown in equations (12)~(15). ξ_1, ξ_2 and ξ_3 are curvilinear coordinates. The coefficients of $c_1 \sim c_{16}$ are determined by substitution of f and its derivatives at the eight vertices of the cell.

$$\begin{aligned} f^{m+1}(i,j,k) &= \left((c_1\Delta\xi_1+c_4\Delta\xi_2+c_7\Delta\xi_3+c_{11})\Delta\xi_1+c_{14}\Delta\xi_2+\frac{\partial f^*}{\partial\xi_1}(i,j,k)\right)\Delta\xi_1 \\ &+\left((c_1\Delta\xi_2+c_5\Delta\xi_1+c_8\Delta\xi_3+c_{12})\Delta\xi_2+c_{15}\Delta\xi_3+\frac{\partial f^*}{\partial\xi_2}(i,j,k)\right)\Delta\xi_2 \\ &+\left((c_3\Delta\xi_3+c_6\Delta\xi_1+c_9\Delta\xi_2+c_{13})\Delta\xi_3+c_{16}\Delta\xi_1+\frac{\partial f^*}{\partial\xi_3}(i,j,k)\right)\Delta\xi_3 \\ &+c_{10}\Delta\xi_1\Delta\xi_2\Delta\xi_3+f^*(i,j,k) \end{aligned} \tag{12}$$

$$\begin{aligned} &\frac{\partial f^{m+1}}{\partial\xi_1}(i,j,k) \\ &=(3\times c_1\Delta\xi_1+2(c_4\Delta\xi_2+c_7\Delta\xi_3+c_{11}))\Delta\xi_1 \\ &+(c_5\Delta\xi_2+c_{10}\Delta\xi_3+c_{14})\Delta\xi_2+(c_6\Delta\xi_3+c_{16})\Delta\xi_3 \\ &+\frac{\partial f^*}{\partial\xi_1}(i,j,k)-\Delta t\left(\frac{\partial f^*}{\partial\xi_1}\frac{\partial U_c}{\partial\xi_1}+\frac{\partial f^*}{\partial\xi_2}\frac{\partial V_c}{\partial\xi_1}+\frac{\partial f^*}{\partial\xi_3}\frac{\partial W_c}{\partial\xi_1}\right) \end{aligned} \tag{13}$$

$$\begin{aligned} &\frac{\partial f^{m+1}}{\partial\xi_2}(i,j,k) \\ &=(3\times c_2\Delta\xi_2+2(c_5\Delta\xi_1+c_8\Delta\xi_3+c_{12}))\Delta\xi_2 \\ &+(c_9\Delta\xi_3+c_{10}\Delta\xi_1+c_{15})\Delta\xi_3+(c_4\Delta\xi_1+c_{14})\Delta\xi_1 \\ &+\frac{\partial f^*}{\partial\xi_2}(i,j,k)-\Delta t\left(\frac{\partial f^*}{\partial\xi_1}\frac{\partial U_c}{\partial\xi_2}+\frac{\partial f^*}{\partial\xi_2}\frac{\partial V_c}{\partial\xi_2}+\frac{\partial f^*}{\partial\xi_3}\frac{\partial W_c}{\partial\xi_2}\right) \end{aligned} \tag{14}$$

$$\begin{aligned} &\frac{\partial f^{m+1}}{\partial\xi_3}(i,j,k) \\ &=(3\times c_3\Delta\xi_3+2(c_6\Delta\xi_1+c_9\Delta\xi_2+c_{13}))\Delta\xi_3 \\ &+(c_7\Delta\xi_1+c_{10}\Delta\xi_2+c_{16})\Delta\xi_1+(c_8\Delta\xi_2+c_{15})\Delta\xi_2 \\ &+\frac{\partial f^*}{\partial\xi_3}(i,j,k)-\Delta t\left(\frac{\partial f^*}{\partial\xi_1}\frac{\partial U_c}{\partial\xi_3}+\frac{\partial f^*}{\partial\xi_2}\frac{\partial V_c}{\partial\xi_3}+\frac{\partial f^*}{\partial\xi_3}\frac{\partial W_c}{\partial\xi_3}\right) \end{aligned} \tag{15}$$

$$\begin{aligned} \Delta\xi_1&=-U_c\Delta t \\ \Delta\xi_2&=-V_c\Delta t \\ \Delta\xi_3&=-W_c\Delta t \end{aligned} \tag{16}$$

where U_c, V_c and W_c are contra-variant velocity components in ξ_1, ξ_2 and ξ_3 directions.

$$\begin{aligned} U_c&=(\xi_1)_x(u-u_g)+(\xi_1)_y(v-v_g)+(\xi_1)_z(w-w_g) \\ V_c&=(\xi_2)_x(u-u_g)+(\xi_2)_y(v-v_g)+(\xi_2)_z(w-w_g) \\ W_c&=(\xi_3)_x(u-u_g)+(\xi_3)_y(v-v_g)+(\xi_3)_z(w-w_g) \end{aligned} \tag{17}$$

4.2 MAC method

The present method is based on the MAC method proposed by Welch et al.(1966). The Poisson equation for pressure includes the divergence of the convection term, which is different from the equation used in the CIP method. The

velocity components at new time step are extrapolated by the Euler explicit scheme. The convection terms and the kinematic free surface boundary condition are discretized by the third order upwind scheme. All the other spatial derivative terms are discretized by the second order centered difference scheme.

5. Pilot Computations

The ship waves calculated by the CIP and MAC methods in deep water were compared with experimental results published by ITTC (1983). The comparison of wave profiles for Wigley hull at Fn=0.289 is shown in Fig. 1. Fn means the Froude number based on the ship length. The minimum grid size in the longitudinal, the lateral, and the vertical direction is 0.005L, 0.002L, and 0.003L, respectively. The number of grids per one wave length in far field is 13 in both cases. The computed wave elevations on the hull are similar to the measured results, but the wave patterns computed by the MAC method are different from that of the CIP method as shown in Fig. 2. The computed wave pattern by the CIP method shows well propagation of wave in far field while that of the MAC method does not so much. Through the comparison of the inviscid flow computations, it is found that CIP method has a merit to predict ship waves accurately in far field.

However, the inviscid flow computations gave the overestimation of the wave height in wake zone as shown in Fig. 2. The main reason of the deviation seems to be viscous effects. In order to confirm the reason for the discrepancy of the stern wave, the viscous flow computations were carried out. The numerical scheme including viscous effect is the same as that of the inviscid flow computation. An algebraic eddy-viscosity model proposed by Baldwin et al.(1987) was used for the turbulence transportation. The model has been widely used for the flow simulation around ships because of its simplicity. In the computation of viscous flow minimum grid size in lateral direction is 0.0003L and number of grid per one wave length is the same as that of the inviscid flow computation.

The comparison of wave patterns between experiment and computations for the viscous flow is displayed in Fig. 3. Rn denotes the Reynolds number based on the ship length. The discrepancy observed in Fig. 2 cannot be found in the viscous flow computations. Through the computations for the viscous flow, it was confirmed that the reason of the discrepancy of stern wave was caused by ignore of the viscous effect.

Remind the introduction of this study. Our

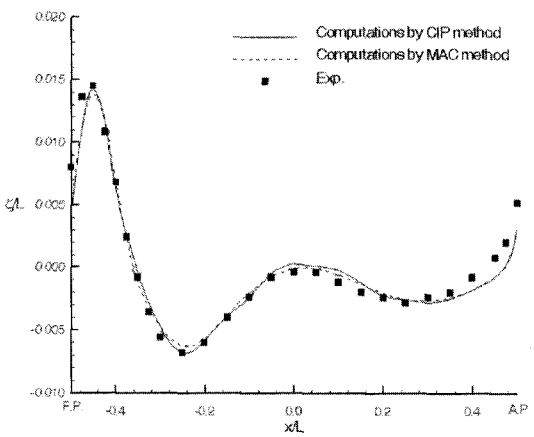

Fig. 1 Comparison of wave profiles on Wigley hull (Fn=0.289)

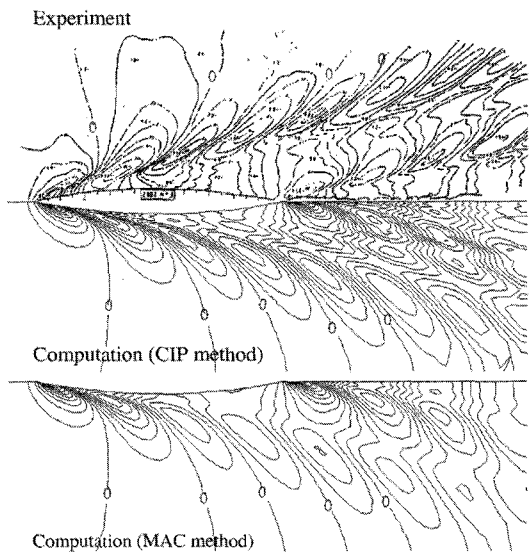

Fig. 2 Comparison of wave patterns between experiment and computation for inviscid flow (Fn=0.289, Interval of contour is 0.00125L)

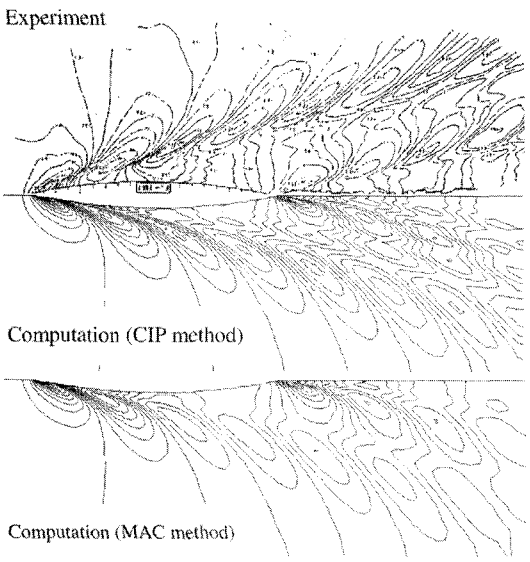

Fig. 3 Comparison of wave patterns between experiment and computation for viscous flow (Fn=0.289, Rn=10^6)

concern was to evaluate the effect of sectional shape of waterway on the ship wave in restricted waterway. The wash impact caused by the divergent wave is more significant than that of the transverse wave. Since the inviscid flow computations gave accurate solution for the divergent wave and the viscous flow computation for required an expensive computational effort, it can be expected that the inviscid flow computation is adequate to achieve our purpose.

6. Results and Discussions

To investigate wave phenomena corresponding to the shape of waterway sections, the computations for three different waterway sections were performed at the critical speed, Fnh=1.0. Fnh denotes the Froude number based on the water depth at the center of waterway. The waterway configurations are shown in Fig. 4. The water depth and width are 0.1L and 1.0L, respectively. Henn et al.(2001) have studied the effect of the bottom shape in shallow water canal. They mentioned that the steep waves were appeared near the side wall at the critical speed. However the steep waves could not be observed in the shore-

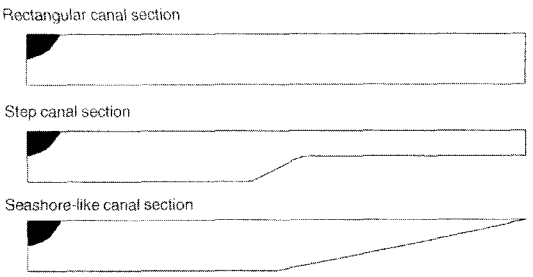

Fig. 4 Configuration of canal section

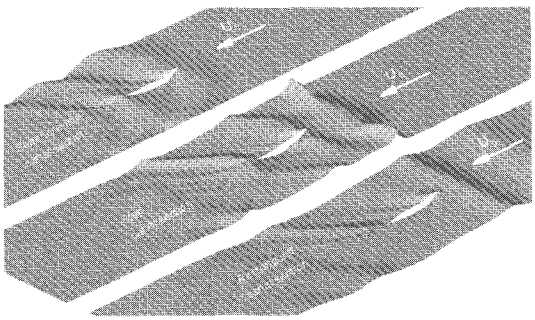

Fig. 5 Wave pattern around Wigley hull according to the canal section (Fnh=1.0, h=0.1L, w=2.0L)

like canal section as shown in Figs. 5 and 7. Fig. 5 shows the perspective view of the ship waves. In rectangular canal section the solitary waves moved ahead with constant wave height over the full canal width, while in the vertical side wall, very steep wave near to the side wall was found. The steep waves were generated by the concentration of the divergent wave. On the other hand, the steep waves around side wall could not be observed in the case of shore-like canal. Since there was no vertical side wall in the shore-like canal, the local depth Froude number became large near to the shore. Because the speed of waves around side wall was much slower than the speed of waves at the centerline, the divergent waves could not be concentrated. That is the main reason why there was no steep wave around the shore wall in the shore-like canal section. The shapes of wave crest lines in the shore-like canal section were different from those in the rectangular and step canal sections. The shapes of wave crest lines in shore-like canal section was convex, while those in rectangular and step canal sections

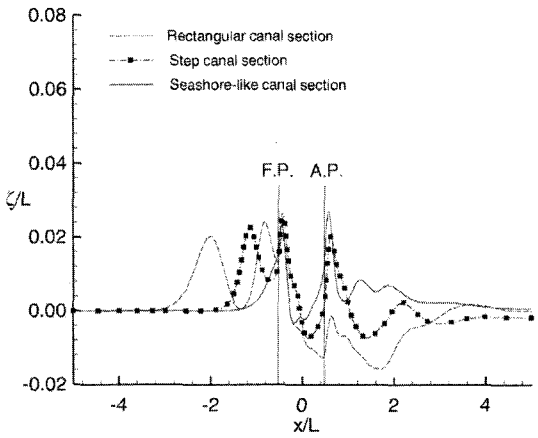

Fig. 6 Wave elevation on the body surface and center plane (Fnh=1.0)

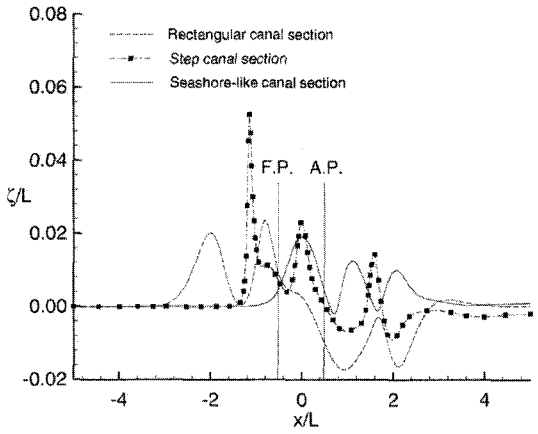

Fig. 7 Wave elevation on the side wall (Fnh=1.0)

were concave or straight.

Figs. 6 and 7 show the wave elevation on the center plane and the side wall. In the case of step canal section, the wave shape around the side wall was most steep and the wave height was largest. This big wave could erode away the bank of river or to make dangerous situation for small boats around the side wall. On the basis of computational results, it was found that the wave phenomena depended on the shape of waterway section and the harmful waves appeared in the step canal section.

7. Conclusions

The CIP method was applied to predict more exact ship waves far from the ship as well as near to the ship. The numerical scheme was validated by the comparison of wave profiles and patterns. The computational results by the CIP method for inviscid flow showed good agreement with measurement except discrepancy of wave height in wake zone. Through the comparison between inviscid and viscous computation, it was found that the difference of stern wave was caused by neglecting viscous effect and the inviscid computation was adequate to evaluate the divergent wave, and the CIP method was better than the MAC method in computational accuracy through the comparison of computational result. The influence of canal shape on wave phenomena was investigated by use of the present method. It was found that the wave phenomena of the shore-like canal section were much different from those of the step or rectangular canal section. The generation of steep solitary waves was found around side wall in the step canal section. It is necessary to compute various cases to find the critical or harmful waves for the further works.

References

Baldwin, B. S. and Lomax, H., 1987, "Thin Layer Approximation and Algebraic Model for Separated Turbulent Flows," *AIAA Paper*, pp. 78~257.

Doctors, L. J., Phillips, S. J. and Day, A. H., 2001, "Focusing the Wave-Wake System of a High-Speed Marine Ferry," *FAST 2001*, pp. 97~106.

Doyle, R., Whittaker, T. J. T. and Elsabar, B., 2001, "A Study of Fast Ferry Wash in Shallow Water," *FAST 2001*, pp. 107~120.

Fukuoka, S., Watanabe, A., Hosokawa, S., Tomari, H. and Kyousai, S., 2000, "Characteristics of a Wave Group Generated by a Tanker in a River and Effect of Detached Break Waters as a Bank Erosion Measure," *J of Hydraulic Eng. in Japan*, Vol. 6, pp. 369~374.

Henn R. and Sharma S. D., 2001, "Influence of Canal Topography on Ship Wave in Shallow Water," *Proc. Of 16th IWWWFB*, pp. 49~52.

Hung, C., 1987, "Extrapolation of Velocity for

Inviscid Solid Boundary Condition," *AIAA J.*, No. 11

ITTC, 1983, "Cooperative Experiments on Wigley Parabolic Models in Japan," *17th ITTC R.C. report*.

Kong, C. Y., Lee, S. M. and Lee, Y. S., 2004, "Composite Overlapping Meshes for the Solution of Radiation Forces on Submerged-Plate," *KSME International Journal*, Vol. 18, No. 7, pp. 1203~1212.

Kong, C. Y., Lee, S. M. and Lee, Y. S., 2004, "A Study on the Modeling of Transitional Lateral Force Acting on the Berthing Ship by CFD," *KSME International Journal*, Vol. 18, No. 7, pp. 1196~1202.

Kwag, S. H., 2000, "Bow Wave Breaking and Viscous Interaction of Stern Wave," *KSME International Journal*, Vol. 14, No. 4, pp. 448~455.

The Maritime and Coastguard Agency, 2001, "A Physical Study of Fast Ferry Wash Characteristics in Shallow Water," *Research project 457*.

Watanabe, Y. and Saeki, H. 1999, "Three-Dimensional Large Eddy Simulation of Breaking Waves," *Coastal Engineering Journal*, Vol. 41, Nos. 3 and 4, pp. 281~301.

Welch, J. E., Harlow, F. H., Shannin, J. P. and Daly, B. J. 1966, "The MAC Method," *Los Alamos Scientific Lab., Report*, LA-3425, Los Alamos, N.W..

Whittaker, T. J. T., Doyle, R. and Elsabar, B., 2001, "An Experimental Investigation of the Physical Characteristics of Fast Ferry," *2nd International euro Conference on High- Performance Marine Vehicles*, pp. 480~491.

Xiao, F., Yabe, T. and Ito, T., 1996, "Constructing Oscillation Preventing Scheme for the Advection Equation by a Rational Function," *Comput. Phys. Commn*, Vol. 93, pp. 1~12.

Yabe, T. and Xiao, F., 1996, "Capturing Free Surface and Universal Treatment of Solid, Liquid, Gas by CIP Method," *Proc. of CFD Symposium for Free Surface Flows*, pp. 119~127.